JOURNAL OF MATERIALS SCIENCE 15 (1980) 2605–2611

Annealing behaviour of amorphous μ-phase alloys of FeW and MoCo

J. L. BRIMHALL, R. WANG, H. E. KISSINGER
Battelle, Pacific Northwest Laboratories, Richland, Washington 99352, USA

Crystallization in sputter deposited, amorphous FeW and MoCo of μ-phase composition alloys has been studied using transmission electron microscopy (TEM), electrical resistivity and X-ray diffraction. The amorphous alloys exhibit high thermal stability and transform directly to the equilibrium μ-phase with no intermediate metastable phase formation. In FeW, a tungsten–iron solid solution also forms as the alloy composition is actually in a two-phase (μ + solid solution) region. In both alloys, the crystallites form on a very fine scale and the μ-phase is heavily faulted. The crystallization behaviour may be indicative of a marked similarity between the short range structure of the amorphous phase and the μ-phase structure. Changes in electrical resistivity during crystallization are in substantial agreement with the structural changes observed through TEM and X-ray analysis.

1. Introduction

A new class of amorphous alloys based on the composition of complex crystal structures such as the μ-phase has recently been made by a high rate sputter deposition, [1, 2]. These alloys consist of a refractory metal and a transition metal, and exhibit high thermal stability against crystallization as measured by differential scanning calorimetry (DSC).

The mechanism of crystallization in these alloys has not been studied, however. Considerable differences could be expected in the crystallization of these amorphous μ-phase alloys as compared to that in rapidly quenched, deep eutectic alloys. Crystallization in eutectic composition alloys generally proceeds through a series of metastable phases to the final equilibrium phases. A principal objective of the study was to determine whether this phenomenon is seen in the amorphous μ-phase alloys. Differences in the crystallization behaviour could also help explain differences in the structural models for these alloys compared to the eutectic type alloys.

2. Experimental techniques

The amorphous alloys were prepared by sputter deposition using high rate triode sputtering. Targets used for sputter deposition were prepared by compacting the respective metal powders under high temperature and pressure. One FeW target was made by imbedding strips of tungsten into a solid block of iron. However, most of the annealing studies utilized the alloys made from the powder compact target. The alloys were deposited at a rate of 0.07 μm sec^{-1} on a substrate cooled by liquid nitrogen. Typical thickness of the final deposit was 200 μm. The composition of the final deposit was 50 at %Fe–50 at %W for the FeW alloy and 54 at %Co–46 at %Mo for the MoCo alloy.

Specimens suitable for transmission electron microscopy (TEM) were cut from the deposited wafer and annealed in a vacuum of 1×10^{-6} torr for various times and temperatures. Specimens were thinned for examination in TEM after annealing. X-ray analysis was also done on the TEM specimens.

The electrical resistivity was measured using the standard four probe technique. Resistivity specimens measuring approximately 1 mm × 10 mm were cut from the original deposits. Accurate values for resistivity were difficult to determine because of non-uniformity of shape. However, the value of ~ 240 μohm cm for amorphous MoCo

0022–2461/80/102605–07 $02.70/0

compares well with other reported resistivity values for amorphous metals [3, 4]. Measurements were made at both room temperature (~ 295 K) and liquid nitrogen temperature (78 K) following 1 h annealing treatments. All measured values were normalized by dividing by the resistivity of the starting amorphous condition. A measure of the temperature coefficient of resistivity was also obtained by comparing the resistivity at 295 K with that at 78 K. In order to protect the very fragile specimens, they were mounted in a protective cage-like enclosure. All anneals and measurements were made without removing the specimen from the mounting.

3. Results

The results on the deposited and annealed microstructures are similar in the two alloys and are reported together below. Both alloys show a featureless amorphous microstructure but there is some indication of recovery and localized ordering upon annealing below the crystallization temperature. Crystallization to the stable μ-phase occurred with no intermediate phase formation. Some differences in behaviour of the two alloys were observed during crystallization, however. These results are, therefore, reported separately.

3.1. As-deposited amorphous structure

The as-deposited microstructure of both FeW and MoCo was completely featureless. In Fig. 1, the selected area diffraction (SAD) patterns show one bright, diffuse ring plus several larger, much fainter rings. These are common observations for amorphous alloys. The formation of these particular amorphous phases was reported previously [1, 2].

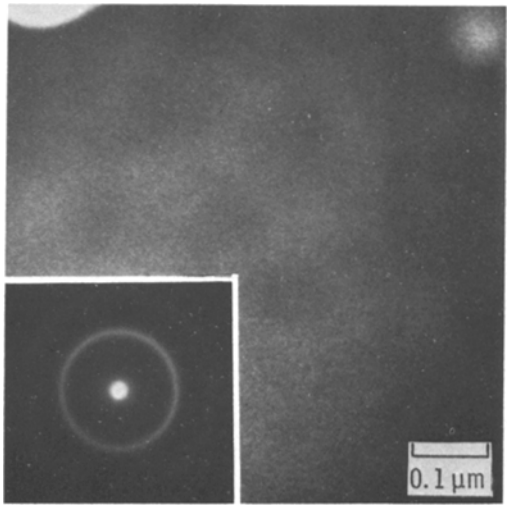

Figure 1 Microstructure of amorphous FeW, as-deposited showing featureless contrast. MoCo has identical appearance.

A distinct difference in the amorphous structure between these alloys and the metal–metalloid eutectic alloys is indicated by comparison of the SAD patterns. The ratio of the diameters of the two outer diffuse rings to the inner ring gives values of 1.66 and 1.97 for FeW and 1.66 and 1.99 for MoCo. Ratios of 1.67 and 1.98 were measured in an amorphous, sputter deposited MoNi alloy. These values were markedly different from those measured in a sputter deposited $Ni_{80}B_{20}$ alloy, 1.72 and 2.27 respectively.

3.2. Annealed, non-crystalline structure

A small but detectable amount of clustering or ordering occurred in the amorphous structure during annealing at temperatures just below the onset of crystallization. These changes were noted by dark field electron microscopy (DF) in which a portion of the first diffuse ring formed the DF image. Such DF images are shown in Fig. 2 and reveal small bright spots 20–50 Å in size. These bright spots represent coherently diffracting domains in the structure such as would be produced by localized ordering [5]. Such bright spots were only barely resolvable in the unannealed material so have definitely increased in size as a result of annealing.

The bright spots or ordered regions do not grow into a recognizable crystalline structure after prolonged annealing, e.g., 48 h at 970 K for FeW. There was no evidence for the formation of a single, truly crystalline phase from these ordered regions.

3.3 Crystallized structure – FeW

Crystals of two different phases were first noted after 8 h at 1120 K, Fig. 3. The globular phase is bcc ($a_o \simeq 0.317$ mm) and predominantly tungsten. The striated phase could not be identified from the SAD patterns but X-ray diffraction showed only a bcc phase and a μ-phase (Fe_7W_6) to be present. It was therefore concluded that the striated phase is the μ-phase.

A completely crystallized structure comprising an intermixture of the bcc tungsten phase and μ-phase formed after 24 h at 1120 K. An almost identical structure is produced after only 1 h

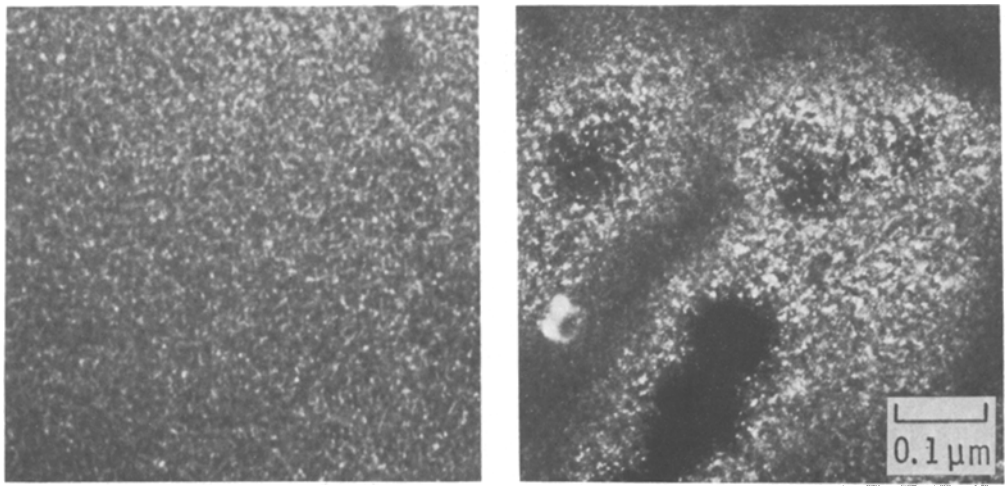

Figure 2 DF micrographs imaged using a small portion of the brightest ring in the SAD pattern. (a) FeW 1 h at 1120 K, (b) MoCo at 970 K. Small coherently diffracting domains are resolvable.

anneal at 1220 K, Fig. 4. Very pronounced streaking is noted in the SAD pattern taken from only the striated μ-phase (centre portion of Fig. 4). This indicates that the twins or platelets in the μ-phase are extremely thin. The fractional amount represented by the two phases is difficult to determine mainly owing to the faintness of the striations in some cases and the fact that twin or platelets parallel to the foil will not appear as striations. A range of 20–50% for the b c c phase would be a crude estimate.

A strong texture in the b c c tungsten phase was a unique feature of the crystalline structure. SAD patterns covering large areas reveal a pronounced (0 0 1) texture in Fig. 5. A different region showed a (0 1 1) texture. No relation of this texture to the faulting in the μ-phase could be discerned as the striations are arrayed randomly among the structure.

An iron–tungsten–carbide phase was the only additional phase observed in the FeW alloy, Fig. 6. The carbides form after annealing at the higher temperatures ($\geq$ 1270 K) and only in the deposit that was made from the powder compact target. The distribution of the carbide phase was very inhomogeneous on a TEM scale. Large areas show no carbides. X-ray diffraction did not reveal the carbide phase, so the total amount is quite small.

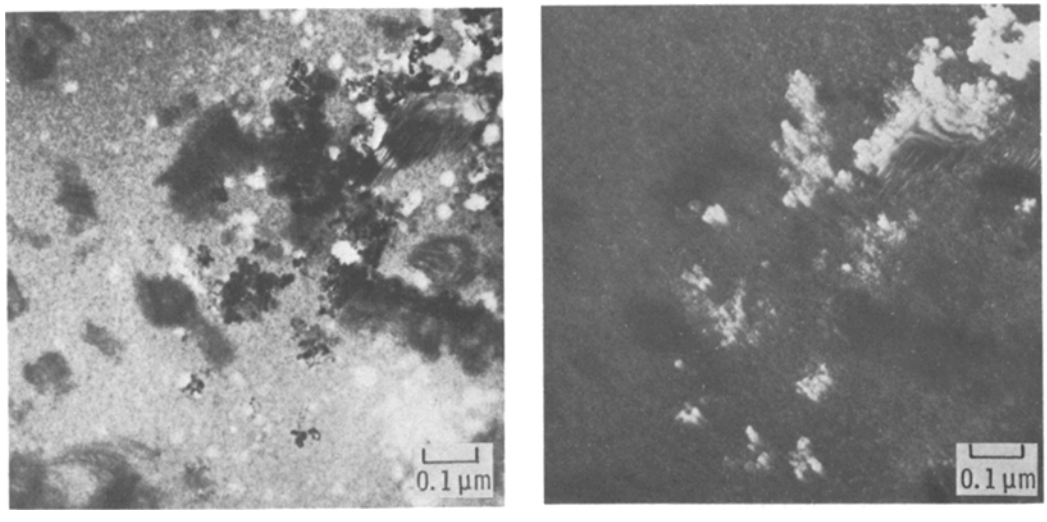

Figure 3 Microstructure of amorphous FeW annealed for 8 h at 1120 K shows a mixture of μ-phase and b c c phase in an amorphous matrix. (a) BF, (b) DF.

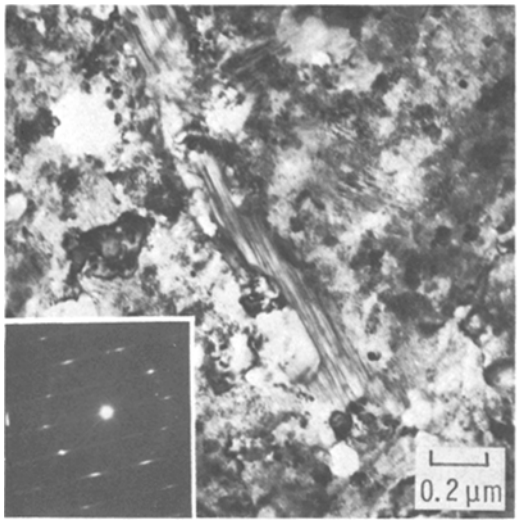

Figure 4 Microstructure of amorphous FeW annealed for 1 h at 1220 K. Structure is completely crystallized. SAD pattern from centre region of the micrograph.

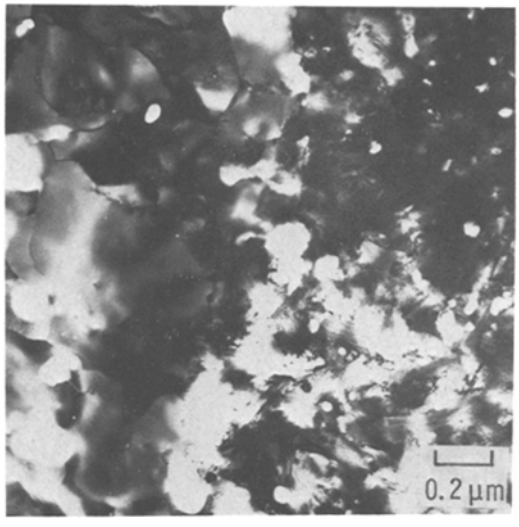

Figure 6 Microstructure of FeW annealed for 2 h at 1270 K. Large iron–tungsten–carbide grains are present on the left.

A somewhat higher crystallization temperature was also observed in the deposit made from the powder compact target indicating that the excess carbon was acting to stabilize the amorphous phase.

The μ-phase grains grew large during annealing at 1270 K for long times and these could be positively identified by SAD patterns. The μ-phase is still heavily faulted, however, as shown in Fig. 7. The lattice parameter of the bcc tungsten increased from 0.3147 nm after 1070 K to 0.3156 nm after 1270 K. Different amounts of iron dissolved in the tungsten could explain this variation. The lattice parameter was always found to be less than pure tungsten.

3.4. Crystallized structure–MoCo

Crystals of MoO_2 were the first phase to appear at temperatures as low as 870 K, Fig. 8. The matrix surrounding the crystals is the recovered amorphous structure illustrated by Fig. 2. The amount of oxide was less than 1% by volume and saturated after several hours of annealing due to a depletion

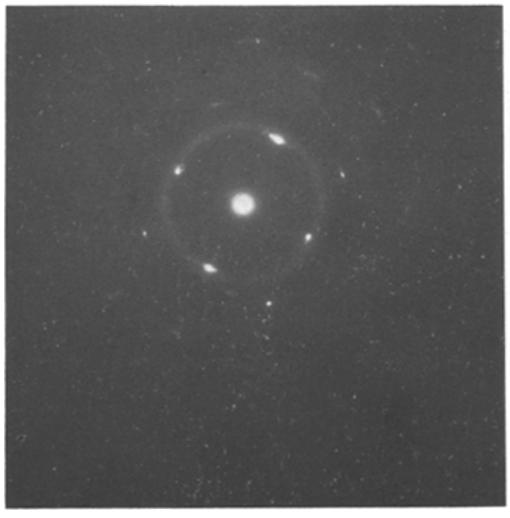

Figure 5 SAD pattern covering very large region of the speciment shown in Fig. 4.

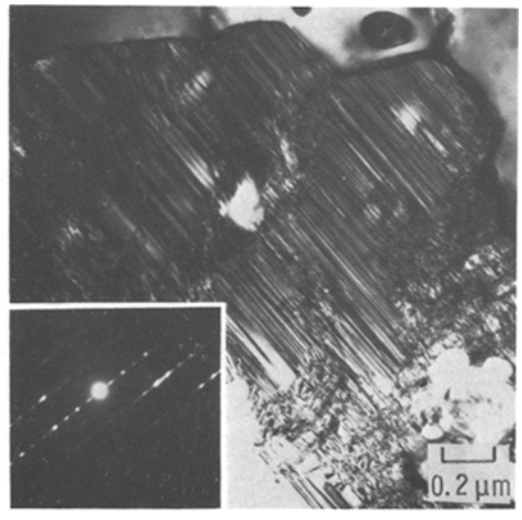

Figure 7 Microstructure of FeW annealed for 24 h at 1270 K. The heavily faulted grain is the μ-phase, Fe_7W_6.

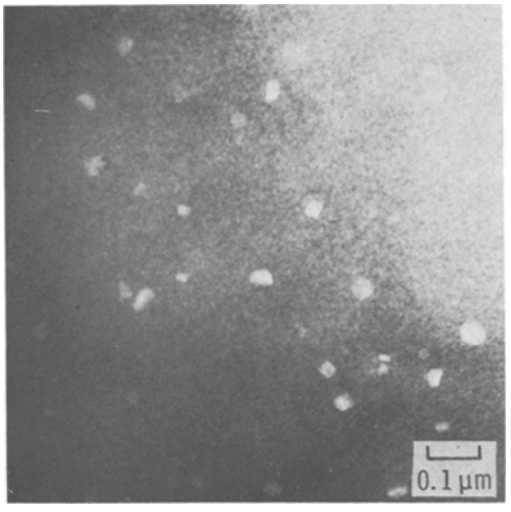

Figure 8 Microstructure of amorphous MoCo annealed for 2 h at 870 K. Particles are MoO_2 embedded in the still amorphous matrix.

of oxygen. No relation between the oxide and subsequent crystallization of metallic phases could be detected.

A partially crystalline structure resulting from a 2 h anneal at 1020 K is shown in Fig. 9. The structure is characterized by a fine crystallite size as shown by the bright field–dark field pair. Lattice spacings consistent with the Mo_6Co_7 μ-phase are given by the spotty rings. No rings consistent with pure Mo could be detected. Some residual amorphous material is indicated by the diffuse background ring. The amorphous material, however, was a minor part of the structure after this annealing treatment.

A uniform, fine, completely crystalline structure was obtained after annealing at 1070 and 1170 K, Fig. 10. Only the μ-phase could be detected by SAD or X-ray analysis. No molybdenum or any other phase was detected. Faulting is observed in the μ-phase grains similar to the μ phase in FeW. Streaking is also present in the SAD pattern similar to that found in FeW.

3.5. Electrical resistivity

A sharp drop in the normalized resistivity values as a function of annealing temperature coincided with the onset of crystallization, Fig. 11. A small but reproducible drop in resistivity was also noted just prior to the large drop indicating that some type of recovery or relaxation process had occurred.

The temperature coefficient of resistivity, indicated by the lower curves in Fig. 11, also correlated well with the crystallization behaviour. A very small temperature coefficient is indicated for the amorphous state but this increases as crystallization proceeds. The metallic tungsten phase in the FeW alloy could be responsible for the peak in that particular curve. No such peak

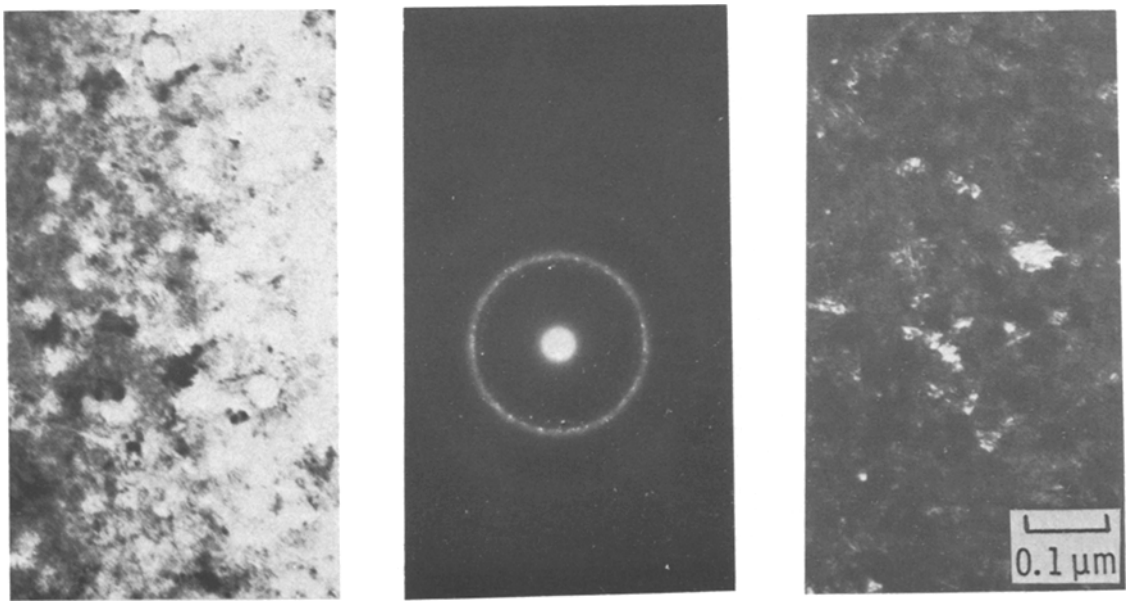

Figure 9 Microstructure of MoCo annealed for 2 h at 1020 K showing formation of fine crystallites. (a) BF, (b) SAD, (c) DF from the spotty ring.

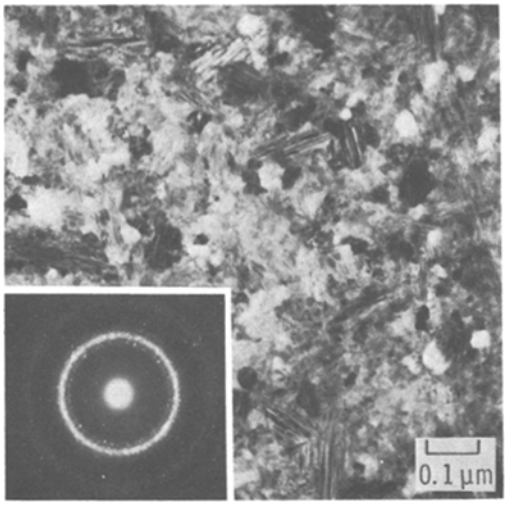

Figure 10 Microstructure of MoCo annealed for 2 h at 1070 K. Structure completely crystallized into μ-phase Mo_6Co_7.

was observed in MoCo and no pure metallic phases were observed.

A lower crystallization temperature at the surface of the amorphous deposit was first detected as a result of the resistivity measurements. Subsequent X-ray analysis revealed that crystallization in the surface region exposed to the substrate began at temperatures 50–70 K below that of the bulk or free surface. Backsputtering of copper from the substrate into the amorphous deposit is believed to be responsible for this phenomenon.

4. Discussion

The crystallization temperatures of these μ-phase amorphous alloys are significantly higher than reported for liquid quenched, eutectic alloys. A 2 h crystallization temperature of ~ 1150 K for FeW and 1000 K for MoCo compares with 880 K for $Nb_{60}Ni_{40}$ and 630 K for an Fe–Ni–P–B alloy [6]. The melting points of elements in the $Nb_{60}Ni_{40}$ alloy are about the same as those in the MoCo alloy yet the $Nb_{60}Ni_{40}$ shows less thermal stability in the amorphous state.

Direct transformation of the amorphous structure to the crystalline μ-phase with no intermediate phase formation is the basic mechanism of crystallization in these alloys. This is a prime example of a polymorphous transformation as described by Herold and Köster [7]. The fine crystallite size also indicates a high degree of crystal nucleation. In many amorphous alloys, isolated crystals tend to grow to a rather extensive

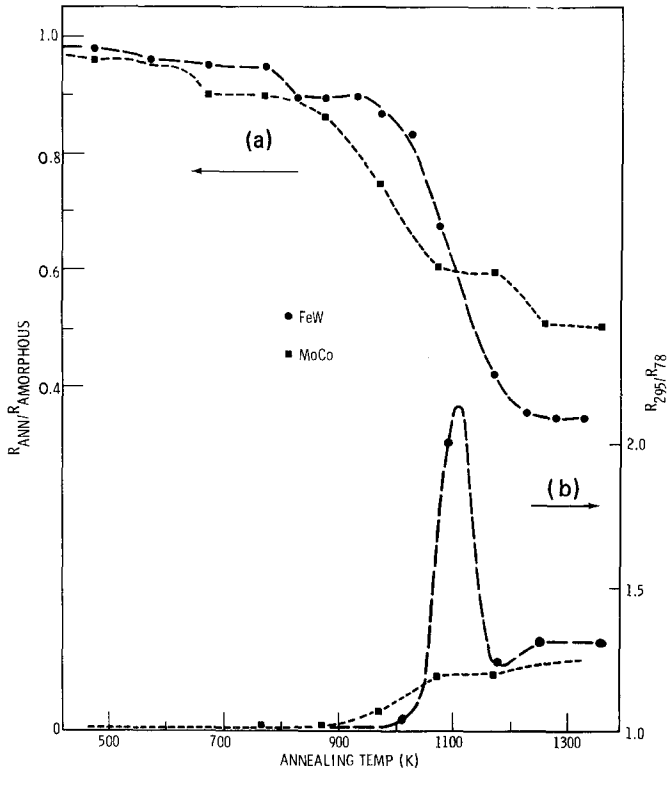

Figure 11 (a) Change in electrical resistivity measured at 78 K as a function of annealing temperature, (b) change in the ratio of resistivity at 295 K to that at 78 K as a function of annealing temperature.

size in an amorphous matrix. Such observations as above suggest a similarity in the short-range order structure of the amorphous phase with the μ-phase crystalline structure, as proposed by Wang [8].

The significant fraction of tungsten in the crystallized FeW alloy results from the alloy composition actually being in a two-phase field. The μ-phase Fe_7W_6 actually contains 60% iron with the excess iron atoms occupying some of the tungsten sites [9]. The amorphous alloy is approximately 50% Fe–50% W, so it is well within the two-phase region. However, direct transformation of both the tungsten and μ-phase from the amorphous state was indicated. The initial precipitation of a tungsten phase would leave excess iron in the amorphous matrix, thereby inducing an easier transformation to the Fe-rich μ-phase.

The observations reported here, therefore, suggest a much simpler crystallization process for the μ-phase alloy than that suggested by Masumoto and Maddin for amorphous alloys [10]. They state and many experiments show that most amorphous metals crystallize through the formation of metastable phases to the final equilibrium phase or phases [10].

Some type of recovery or atomic rearrangement must be occurring to account for the slight drop in resistivity prior to crystallization. Structural relaxation prior to crystallization has been reported in amorphous metal alloys [11, 12]. This drop in resistivity could be a manifestation of the same process that produces the coherently diffracting domains observed in dark field micrographs. Whether such domains actually serve as crystal nuclei was not determinable owing to the rapid nucleation when crystallization occurred. It is certainly quite feasible that they can be the crystal nuclei, however.

No incipient stage of crystallization is observed in these alloys in which a single phase, simple structure (bcc or fcc) emerges from the amorphous state with no apparent nucleation stage. This has been observed in a number of amorphous alloys after long, low temperature annealing [10, 13, 14]. Since Fe and W both have bcc structures in their elemental stage, such a phenomenon might have been expected but there was no evidence of it after 48 h at 970 K.

The appearance of oxide and carbide phases emphasizes the importance of target material purity in preparing amorphous alloys by sputter deposition. These phases did not seem to affect the crystallization behaviour, on the basis of the limited results obtained. The increase in thermal stability due to carbon is consistent with other results in which impurities stabilize the amorphous phases [15]. Since oxygen free MoCo was not obtained, it is difficult to say whether oxygen does the same.

5. Conclusions

The important conclusions are summarized as follows.

(1) Amorphous alloys of FeW and MoCo with μ-phase compositions show very high thermal stability.

(2) Crystallization occurs by direct transformation to the equilibrium crystalline phase.

(3) The annealing behaviour suggests a close similarity between short range order in amorphous structure and the μ-phase structure.

(4) Changes in electrical resistivity correlate well with observed changes in microstructures.

References

1. R. WANG, M. D. MERZ, J. L. BRIMHALL and S. D. DAHLGREN, "Rapidly Quenched Metals III", Vol 1 (Metals Society, London, 1978) p. 420.
2. *Idem, Scripta Met.* **12** (1978) 1037.
3. H. J. GÜNTHERODT and H. U. KÜNZI, "Metallic Glasses" (American Society for Metals, Metals Park, Ohio, 1978) 247.
4. A. M. STEWART and W. A. PHILLIPS, *Phil. Mag.* **B37** (1978) 561.
5. P. CHAUDARI, J. F. GRACZYK and J. R. HERD, *Phys. Stat. Sol. (b)* **51** (1972) 801.
6. B. G. LEWIS, H. A. DAVIES and K. D. WARD, *Scripta Met.* **13** (1979) 313.
7. V. HEROLD and V. KÖSTER, "Rapidly Quenched Metals III", Vol 1 (Metals Society, London, 1978) p. 281.
8. R. WANG, *Nature* **78** (1979) 700.
9. A. RAMAN, *Z. Metall.* **57** (1966) 301.
10. T. MASUMOTO and R. MADDIN, *Mater. Sci. and Eng.* **19** (1975) 1.
11. A. J. KEARNS, D. E. POLK, R. RAY and B. C. GIESSEN, *ibid.* **38** (1979) 49.
12. T. EGAMI, *Mater. Res. Bull.* **13** (1978) 557.
13. T. MASUMOTO and R. MADDIN, *Acta Met.* **19** (1971) 725.
14. A. REVLOLESCHI and N. J. GRANT, *Met. Trans.* **3** (1972) 1545.
15. M. R. BENNETT and J. G. WRIGHT, *Phys. Stat. Sol. (a)* **13** (1972) 135.

Received 20 February and accepted 20 March 1980.